Functional Proteomics: Examining the Effects of Hypoxia on the Cytotrophoblast Protein Repertoire†

Van M. Hoang,‡ Russell Foulk,# Karl Clauser,× Alma Burlingame,§,|| Bradford W. Gibson,§,||,⊥ and Susan J. Fisher*,§,¶,∞,▽

Graduate Program in Pharmaceutical Chemistry, Departments of Pharmaceutical Chemistry, Chemistry and Chemical Biology, Pharmaceutical Sciences and Pharmacogenomics, Stomatology, Anatomy, and Obstetrics, Gynecology and Reproductive Sciences, University of California San Francisco, San Francisco, California 94143, Department of Obstetrics and Gynecology, University of Nevada, Reno, Nevada 89509, and Department of Protein Sciences, Millenium Pharmaceuticals Inc., Cambridge, Massachusetts 02139

Received October 16, 2000; Revised Manuscript Received February 4, 2001

ABSTRACT: The outcome of human pregnancy depends on the differentiation of cytotrophoblasts, specialized placental cells that physically connect the embryo/fetus to the mother. As cytotrophoblasts differentiate, they acquire tumor-like characteristics that enable them to invade the uterus. In a novel feedback loop, the increasingly higher levels of oxygen they encounter within the uterine wall influence their differentiation into vascular-like cells. Together, the invasive and cell surface properties of cytotrophoblasts enable them to form vascular connections with uterine blood vessels that divert maternal blood flow to the placenta, a critical hurdle in pregnancy. It is therefore important to understand how cytotrophoblasts respond to changes in oxygen tension. Here we used a proteomics approach, two-dimensional polyacrylamide gel electrophoresis (2-D PAGE) combined with mass spectrometry, to characterize the protein repertoire of first trimester human cytotrophoblasts that were maintained under standard tissue culture conditions (20% O_2). 2-D PAGE showed a unique protein map as compared to placental fibroblasts and human JEG-3 choriocarcinoma cells. Mass spectrometry allowed the identification of 43 spots on the cytotrophoblast map. Enzymes involved in glycolysis and responses to oxidative stress, as well as the 14-3-3 signaling/adapter proteins, were particularly abundant. Hypoxia in vitro (2% O_2) produced discrete changes in the expression of a subset of proteins in all the aforementioned functional categories. Together, these data offer new information about the early gestation cytotrophoblast protein repertoire and the generalized mechanisms the cells use to respond to changes in oxygen tension at the maternal−fetal interface.

The human placenta plays a critical role in pregnancy outcome. Before birth, this transient organ connects the embryo/fetus to the uterus. This vital connection is made by cytotrophoblasts, specialized epithelial cells of fetal origin that are allocated to the extraembryonic lineage. During normal placentation, a subpopulation of cytotrophoblast stem cells that resides within the placenta differentiates to assume an unusual phenotype that is commonly associated with tumor cells. During this differentiation process, aggregates of cytotrophoblasts attach to, then invade the uterine wall (see diagram in Figure 1, panel A, and photomicrographs in Figure 1, panel B). The interstitial component of invasion extends through the uterine lining (decidua) into the first third of the muscular wall (myometrium). The endovascular component of invasion allows cytotrophoblasts within the uterine wall to breach the resident maternal vessels. Eventually, these fetal cells replace the endothelial lining and a portion of the muscular wall of uterine spiral arteries and, to a lesser extent, veins. This process greatly expands the diameter of these vessels and diverts the flow of maternal blood to the placenta (see arrows, Figure 1, panel A), where gas, waste, and nutrient exchange occur. During pregnancy, this novel chimeric circulatory system, composed of maternal vascular cells and embryonic/fetal cytotrophoblasts, must respond in a dynamic fashion to the ever-increasing demands of the growing fetus for maternal blood.

Given the complexities inherent in cytotrophoblast differentiation, it is not surprising that this process sometimes goes awry, producing a spectrum of placental pathologies and attendant pregnancy complications (reviewed in ref *1*). For example, shallow invasion is associated with preeclamp-

† This work was supported by grants from the National Institutes of Health (HD30367 and RR 01614).

* To whom correspondence should be addressed. Susan Fisher, HSW 604, University of California San Francisco, San Francisco, CA 94143-0512. Telephone: (415) 476-5297. Fax: (415) 502-7338. E-mail: sfisher@cgl.ucsf.edu.

‡ Graduate Program in Pharmaceutical Chemistry, University of California San Francisco.

§ Department of Pharmaceutical Chemistry, University of California San Francisco.

|| Department of Chemistry and Chemical Biology, University of California San Francisco.

⊥ Department of Pharmaceutical Sciences and Pharmacogenomics, University of California San Francisco.

¶ Department of Stomatology, University of California San Francisco.

∞ Department of Anatomy, University of California San Francisco.

▽ Department of Obstetrics, Gynecology and Reproductive Sciences, University of California San Francisco.

Department of Obstetrics and Gynecology, University of Nevada.

× Millenium Pharmaceuticals Inc.

10.1021/bi0023910 CCC: $20.00 © 2001 American Chemical Society
Published on Web 03/08/2001

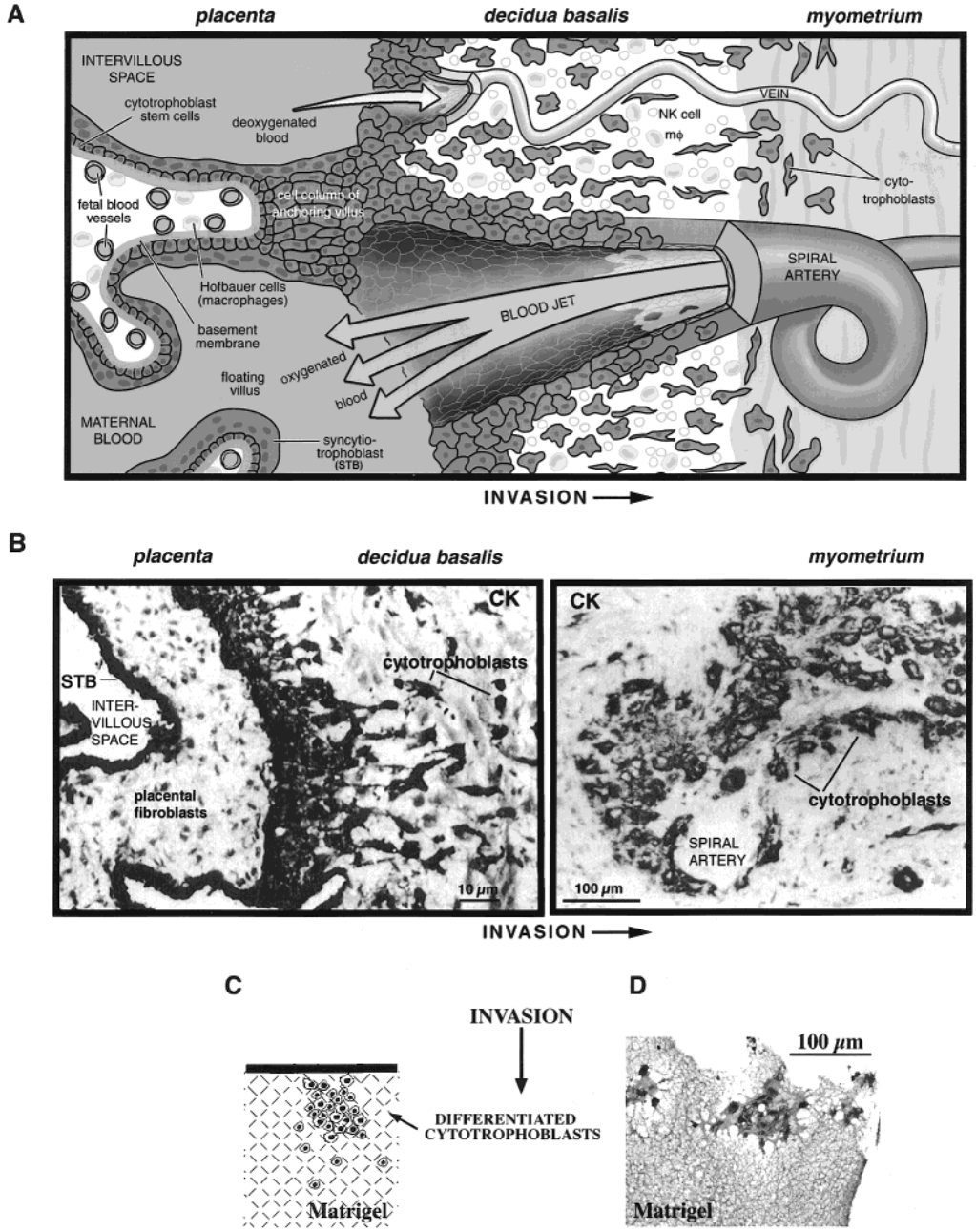

FIGURE 1: Human placental cytotrophoblast differentiation in vivo and in vitro. (A) Diagram depicts the human maternal−fetal interface at mid-gestation. In this location, specialized epithelial cells of the placenta (cytotrophoblasts) differentiate into tumor-like cells that invade the uterine wall and breach maternal blood vessels. Here these placental cells upregulate the expression of adhesion molecules and receptor tyrosine kinases that are usually found on the endothelial cell surface. (B) Tissue sections of the maternal−fetal interface cut from a biopsy of the area diagrammed in panel A. In the photomicrograph on the left, cytokeratin (CK) staining identifies cytotrophoblasts that are emerging from a placental villus and invading the uterine wall. The photomicrograph on the right shows cytotrophoblasts that replaced the maternal cells in the wall of a uterine spiral arteriole. Both panels were adapted from work published by this laboratory (*47*). (C and D) Cytotrophoblast differentiation along the invasive pathway in vitro. This process is diagrammed in panel C and a photomicrograph of a typical culture is shown in panel D. Cytotrophoblast stem cells that are isolated from first trimester placentas and plated on a Matrigel substrate undergo the same differentiation process that is observed during uterine invasion in situ. By 48 h, they are embedded within the substrate.

sia, a syndrome characterized by the sudden onset of maternal hypertension and the appearance of proteinuria and edema during pregnancy (*2*). However, these findings are part of a multisystemic disease that reduces perfusion to virtually all organs in the body (*3*, *4*). Shallow invasion is also associated with a significant percentage of pregnancies that are complicated by fetal intrauterine growth restriction without evidence of maternal preeclampsia. Conversely, cytotrophoblast invasion beyond the normal, tightly circumscribed boundaries occurs to a varying degree in a number of pathological conditions, of which the most aggressive is malignant transformation into choriocarcinoma.

A great deal has been learned about normal cytotrophoblast differentiation by in situ immunolocalization of candidate molecules on tissue sections of the maternal−fetal interface (e.g., Figure 1, panel B). Because isolated stem cells plated on extracellular matrix substrates recapitulate the differentiation process that leads to invasion in vivo (see diagram in

Figure 1, panel C, and photomicrograph in Figure 1, panel D), this culture model has been used to study the function of candidate regulatory molecules. Data generated by using a combination of in situ and in vitro approaches have led to a better understanding of placental development at a molecular level. For example, cytotrophoblast differentiation is governed by an interesting set of transcription factors and their downstream targets. Among the transcription factors with known actions are both positive and negative regulators of the basic helix−loop−helix family (*5*, *6*) and the novel factor glial cells missing (*7*). Downstream targets include a number of stage-specific antigens, such as adhesion molecules, that allow cytotrophoblasts to mimic the surface of endothelial cells (*8*), and proteinases that likely play a role in invasion (*9*). Among the most interesting antigens in this category are molecules that protect cytotrophoblasts within the uterine wall from the immune response typically elicited in transplant situations by other hemiallogeneic cells. These include HLA-G, a major histocompatibility complex class Ib molecule (*10*).

In comparison to published information about the properties of normal cytotrophoblasts, relatively little is known about the effects of pregnancy complications on these cells. With regard to shallow invasion in preeclampsia, cytotrophoblasts within the uterine wall fail to correctly modulate the expression of a number of stage-specific antigens, many of which are related to the acquisition of an adhesion molecule repertoire that is usually associated with vascular cells (*11*). Interestingly, some aspects of the phenotype of cytotrophoblasts in preeclampsia can be replicated in vitro by culturing the cells under hypoxic conditions (*12*, *13*). Together, these observations suggest the hypothesis that abnormal differentiation and hypoxia are critical components of the pathway that leads to this syndrome. With regard to excessive invasion in choriocarcinoma, much of the existing information lies at the genetic level (*14*).

What approaches can be used to obtain new information about the pathways and the processes that are critical to both normal and abnormal placental development? The growing number of transgenic mice that have been generated to study the intraembryonic functions of particular molecules, but yielded placental phenotypes instead (*15*), illustrates the difficulties inherent in candidate single-molecule approaches. Conversely, gene array technologies often identify many more candidate molecules than it is feasible to study (*16*). Here we used a proteomics approach, two-dimensional polyacrylamide gel electrophoresis (2-D PAGE)[1] coupled with mass spectrometry (MS), to map cytotrophoblast protein expression at a global level in normal pregnancy. We also examined the effects of hypoxia in vitro as a model of preeclampsia and other pregnancy complications that are associated with a reduction in blood flow to the placenta. The results showed that major cytotrophoblast proteins normally include an interesting set of molecules that are involved in carrying out glycolysis and handling oxidative stress. In addition, the 14-3-3 signaling proteins are abundant. Of note was the fact that the cytotrophoblast 2-D PAGE map, which was very different from that of placental fibroblasts, bore a greater resemblance to that of the JEG-3 human choriocarcinoma cell line. Hypoxia produced discrete changes in the cytotrophoblast protein repertoire and resulted in nuclear localization of 14-3-3-epsilon. Together, our results suggest that the intracellular cytotrophoblast milieu is specially adapted to handle fluctuations in the cells' metabolic state and oxygen environment as they invade the uterus and form vascular connections with the maternal vessels.

MATERIALS AND METHODS

Materials. Matrigel and Dispase were from Becton-Dickinson (Bedford, MA). Nutridoma-HU was obtained from Boehringer Mannheim Biochemicals (Indianapolis, IN). Millicell-CM cell culture inserts (12 mm) were from Millipore Corporation (Bedford, MA). Bio-Rad Protein Assay reagent was from Bio-Rad (Hercules, CA). Immobiline Drystrips and Pharmalyte pH 3−10 were from Amersham Pharmacia Biotech (Piscataway, NJ). Fast-stain was acquired from Zoion Research (Shrewsbury, MA). Sequencing grade modified trypsin was obtained from Promega (Madison, WI). α-Cyano-4-hydroxycinnamic acid was from Hewlett-Packard (Böblingen, Germany). Nitrocellulose membranes (0.45 μm) were obtained from Schleicher & Schuell (Keene, NH). Rabbit polyclonal antibodies to 1-Cys peroxiredoxin and purified recombinant 1-Cys peroxiredoxin were the kind gift of Dr. Vladimir I. Novoselov (Russian Academy of Sciences, Pushchino, Russia) (*17*). A mouse monoclonal antibody to annexin II and lysates of MDCK cells were from Zymed Laboratories, Inc. (South San Francisco, CA). A rat monoclonal antibody to cytokeratin (*18*) and a mouse monoclonal antibody to HLA-G (*10*) were produced in this laboratory. Affinity-purified rabbit polyclonal antibodies to 14-3-3 epsilon and zeta were from Santa Cruz Biotechnology, Inc. (Santa Cruz, CA). Horseradish peroxidase-conjugated donkey anti-mouse IgG (heavy and light chains), horseradish peroxidase-conjugated donkey anti-rabbit IgG (heavy and light chains), biotin-conjugated donkey anti-rabbit IgG (heavy and light chains), ChromPure donkey IgG (whole molecule), and rhodamine-conjugated donkey anti-rat IgG (heavy and light chains) were from Jackson Immuno Research Laboratories Inc. (West Grove, PA). Enhanced chemiluminescence (ECL) kits were from Amersham Pharmacia Biotech. Avidin/biotin blocking kits, fluorescein-conjugated streptavidin, and Vectashield were from Vector Laboratories, Inc. (Burlingame, CA). All other reagents were acquired from Sigma Chemical Co. (St. Louis, MO).

Cell Culture. Placentas were obtained immediately after first trimester terminations (8−12 wk). Cytotrophoblasts were isolated from pools of multiple placentas by published methods (*9*). Fibroblast contamination, as measured by staining with an anti-vimentin antibody, was ≤5%. The resulting cells were plated on a Matrigel substrate (∼100 μm thick) in serum-free medium (Dulbecco's modified Eagle's medium with 2% Nutridoma-HU, 1% glutamine, and 50 μg/mL gentamycin). The cultured cells were maintained as previously described under either standard tissue culture conditions (5% CO_2/95% air) or in hypoxia (2% O_2/5% CO_2/93% N_2) (*12*). After 48 h, cells were released from the

[1] Abbreviations: 2-D PAGE, two-dimensional polyacrylamide gel electrophoresis; MS, mass spectrometry; ECL, enhanced chemiluminescence; PBS-CMF, calcium- and magnesium-free phosphate buffered saline; T-PBS, PBS-CMF containing 0.1% Tween-20; MALDI-TOF MS, matrix-assisted laser desorption/ionization time-of-flight mass spectrometry; HPLC, high performance liquid chromatography; PSD, postsource decay; Mn SOD, manganese superoxide dismutase; AOE, antioxidant enzyme.

Matrigel by treatment with Dispase and isolated by centrifugation (8 min, 400*g*) in a Sorvall RT 6000D centrifuge (Kendro Laboratory Products, Newtown, CT). The cell pellets were washed three times with Ca^{2+}- and Mg^{2+}-free phosphate-buffered saline (PBS−CMF) and frozen as a pellet prior to lysis.

Anchoring villi were prepared and cultured for up to 3 days as previously described (*19*, *20*) in either standard conditions (20% O_2) or hypoxia (2% O_2) (*13*). Fibroblasts, isolated from first trimester placentas as previously described (*21*), were used after the third passage to ensure that contaminating cells were no longer present. The cells were cultured in Dulbecco's modified Eagle's medium with 10% fetal bovine serum, 1% glutamine, and 50 μg/mL gentamycin. The JEG-3 choriocarcinoma cell line was obtained from the American Type Culture Collection (Manassas, VA) and maintained in Eagle's Minimal Essential Medium with Earle's salts, 1% L-glutamine and 10% fetal calf serum. When confluent, both fibroblasts and JEG-3 cells were released from the substrate with Dispase and isolated by centrifugation. The cell pellets were washed three times with PBS−CMF and frozen prior to lysis.

2-D Polyacrylamide Gel Electrophoresis. Cells were lysed in protein extraction buffer (7 M urea, 2 M thiourea, 4% (3-[(3-cholamidopropyl)dimethylammonio]-1-propanesulfonate), 100 mM dithiothreitol and 1% Pharmalyte pH 3−10), and lysates were centrifuged at 356,000*g* for 10 min in a Beckman Optima TL Tabletop Ultracentrifuge (Beckman Instruments Inc., Palo Alto, CA). The supernatant was removed, and the protein concentration of the extracts was determined by using the Bio-Rad Protein Assay reagent (*22*). Immobiline DryStrips (180 mm, pH 3−10 L) were rehydrated overnight in 400 μL of lysate that contained 250 μg of protein. Isoelectric focusing on a Multiphor II system (Amersham Pharmacia Biotech) and SDS−PAGE on 10% gels using the Investigator System (Genomic Solutions, Chelmsford, MA) were carried out as previously described (*23*). Proteins were visualized using Fast-stain, a modified Coomassie blue stain with increased sensitivity. Digital images of the 2-D PAGE maps were acquired using a Sharp JX-330 desktop scanning unit. The gels were analyzed with the ImageMaster 2D v 2.0 software from Amersham Pharmacia Biotech. Protein spot comparisons were done according to prescribed software instructions. Briefly, the computer program identified protein spots from the digitized images of the gels. In all cases, spot identification was verified by visual inspection. Then we used the software program to compare spots from different gels. Background staining, the average intensity of bordering pixels, was subtracted from the volume measurements of the gel spots.

In-Gel Trypsin Digestion of Proteins and Mass Spectrometry. After gels were destained in 10% acetic acid, protein spots were excised and macerated with a scalpel. In-gel trypsin digests were performed as previously described (*24*). Portions (typically 1/20th) of the unseparated tryptic digests were cocrystallized in a matrix of α-cyano-4-hydroxycinnamic acid and analyzed by using a PerSeptive Biosystems matrix-assisted laser desorption/ionization time-of-flight (MALDI-TOF) DE-STR mass spectrometer equipped with delayed extraction operated in the reflector mode. Spectra were internally calibrated using trypsin autoproteolysis peaks, and the accuracy of mass measurements of all peptides was in the range of ± 0.05 Da. For samples that required peptide separation by high performance liquid chromatography (HPLC), an Eldex Micropro pump was used. Chromatographic runs were performed on a Michrom Bioresources MagicMS C18 column (0.2 × 50 mm; 5 μm particle size; 200 Å pore size) using a flow rate of 1 μL/min. The column was equilibrated with 7% acetonitrile/0.1% trifluoroacetic acid in H_2O. Peptides were eluted isocratically for 10 min followed by a linear gradient (0.95%/min) to a final mobile phase composition of 63% acetonitrile/0.082% trifluoroacetic acid in H_2O. Eluting peptides were detected with an ABI 785A UV detector equipped with a low volume Z cell (Applied Biosystems, Foster City, CA). HPLC fractions of 1−2 μL were spotted directly onto a MALDI target with 1.5 μL of α-cyano-4-hydroxycinnamic acid. Postsource decay (PSD) sequencing was done as previously described (*24*). MS and PSD spectra were interpreted to yield protein identities using the MS-Fit and MS-Tag programs (http://prospector.ucsf.edu).

Immunoblotting. The amount of protein in cell lysates prepared from cytotrophoblasts cultured as described above under standard and hypoxic conditions was estimated by densitometry. Briefly, samples were separated by 1-D PAGE on 10% SDS bis/acrylamide gels and bands were visualized by using Fast-stain. Digital images of the gels were acquired with a Sharp JX-330 desktop scanning unit, and then the intensities of all the pixels in each lane were summed using ImageMaster 2D software. Background staining, the average intensity of bordering pixels, was subtracted from the volume measurements of each lane.

Portions of the cell lysates that contained equal amounts of protein were subjected to 10% SDS−PAGE and then transferred onto nitrocellulose membranes. Immunoblotting was performed as previously described (*6*). Primary antibodies were diluted (v/v) at the ratios indicated: anti-1-Cys peroxiredoxin (1:1000), anti-annexin II (1:1000), anti-14-3-3 epsilon (1:500), anti-14-3-3 zeta (1:500), and anti-HLA-G (1:200). Horseradish peroxidase-conjugated donkey anti-mouse IgG (diluted 1:4000 in blocking buffer) was used to detect anti-annexin II and anti-HLA-G. Horseradish peroxidase-conjugated donkey anti-rabbit IgG (diluted 1:4000 in blocking buffer) was used to detect anti-1-Cys peroxiredoxin and anti-14-3-3 epsilon and zeta. Membranes were processed for chemiluminescence with ECL detection kits according to the manufacturer's instructions. ImageMaster 2D software was used as described above to measure band intensities for comparison purposes. Finally, HLA-G levels, which are not regulated by oxygen tension, were used as a second independent method for estimating the amount of protein that was transferred to each lane of the blot (*6*).

Immunohistochemistry. Villus explants, cultured as described above under either standard or hypoxic conditions, were fixed, embedded, and sectioned as previously reported (*13*). Double indirect immunofluorescence was performed as follows. Nonspecific reactivity was blocked by using a kit from Vector Laboratories according to the manufacturer's instructions. Tissue sections were incubated overnight at 4 °C in antibodies specific to cytokeratin (diluted 1:50 [v/v] in PBS), 14-3-3 epsilon (diluted 1:100 [v/v] in PBS) or 14-3-3 zeta (diluted 1:100 [v/v] in PBS). After washing in PBS, sections were exposed to rhodamine-conjugated donkey anti-rat IgG (diluted 1:200 [v/v] in PBS−CMF) and biotin-

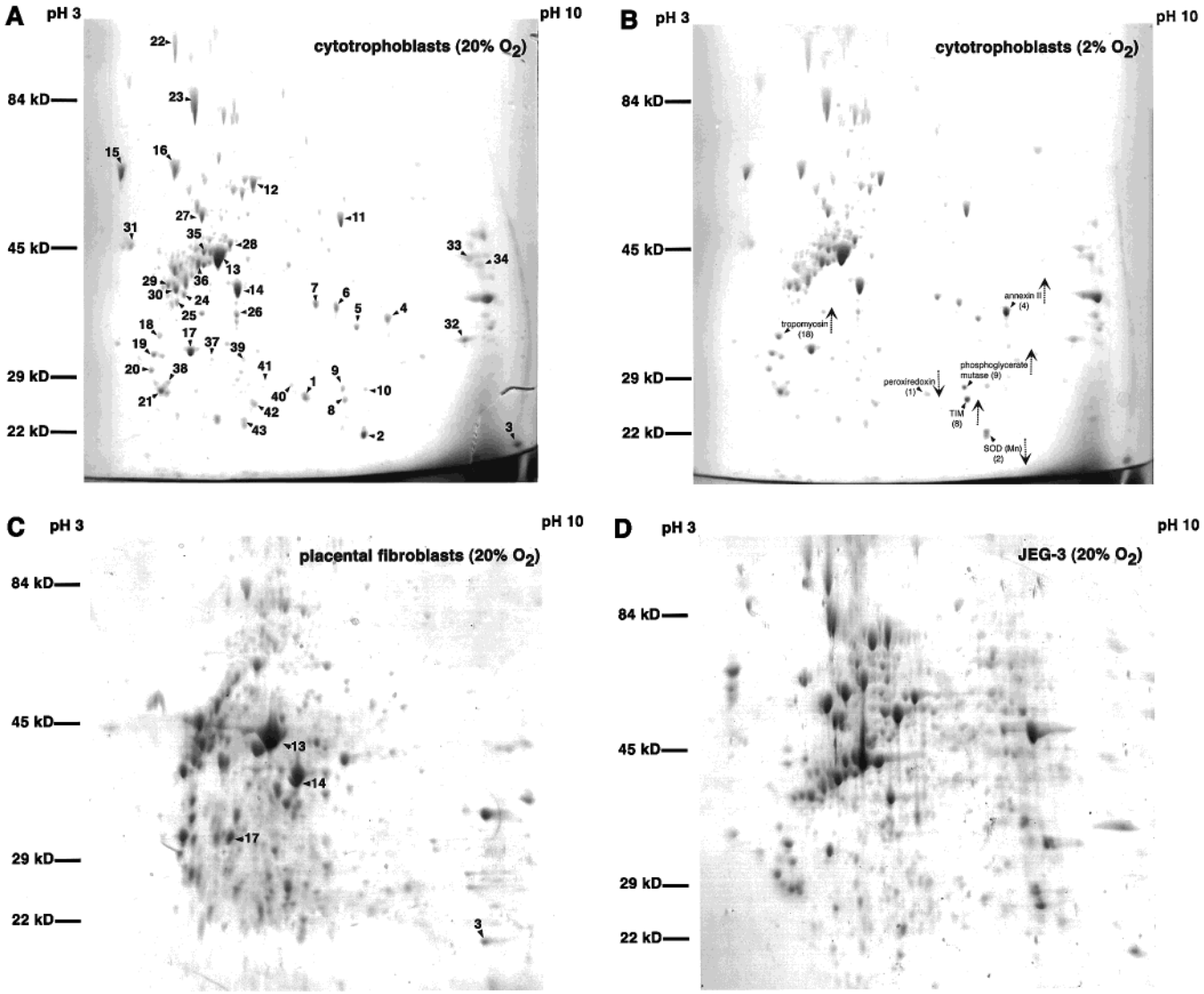

FIGURE 2: 2-D PAGE allowed identification of a subset of first trimester cytotrophoblast proteins that were oxygen regulated. (A and B) 2-D PAGE of lysates that were prepared from cytotrophoblasts cultured for 48 h in 20 or 2% O_2, respectively. (C) Under both conditions, the pattern of cytotrophoblast spots bore little resemblance to that of placental fibroblasts, the other major cell type found in this organ (see Figure 1, panels A and B). (D) In contrast, similarities existed between certain regions of the cytotrophoblast and JEG-3 choriocarcinoma maps (compare with panels A and B). Visual inspection, verified by analyses using Image Master 2D software (see Materials and Methods), suggested that the cytotrophoblast protein repertoire is largely stable in hypoxia; the abundance of six spots changed. Dashed arrows pointing upward indicate increased protein levels in hypoxia. Dashed arrows pointing downward indicate a decrease in protein levels in hypoxia.

conjugated donkey anti-mouse IgG (diluted 1:200 [v/v] in PBS−CMF) for 30 min at 37 °C. Slides were washed and incubated with fluorescein-conjugated streptavidin (diluted 1:200 [v/v] in PBS−CMF) at 37 °C for 15 min. After washing, sections were mounted with Vectashield. Antibody reactivity was visualized by dual channel fluorescence imaging. As a control, the expression of each antigen was evaluated separately on adjacent sections to rule out the possibility of overlap of the emission spectra. Additional controls included omission of either the primary or secondary antibodies.

RESULTS

2-D PAGE. We began by mapping the protein repertoire of cytotrophoblasts cultured under standard conditions (Figure 2, panel A). After staining, the number of spots was estimated by using ImageMaster 2D software; approximately 250 spots were resolved. Since the analysis focused on primary cells, we also investigated whether there were substantial individual variations in the protein components of cytotrophoblast lysates prepared from different placentas, a possible confounding factor for interpreting the results of subsequent experiments that investigated the effects of hypoxia on these cells. Accordingly, this experiment was repeated three additional times. No substantial variations in the repertoire or intensity of protein spots was detected, suggesting that the map shown in Figure 2, panel A, accurately reflected the cytotrophoblast protein repertoire within the confines of the analytical parameters of this experiment.

We also investigated whether the cytotrophoblast protein map was different from or similar to that of fibroblasts, the other major cell type found in the placenta. The fibroblasts that form the stromal cores of chorionic villi (see photomicrograph in Figure 1, panel B) yielded a very different protein map (Figure 2, panel C). A few major proteins, such as spots

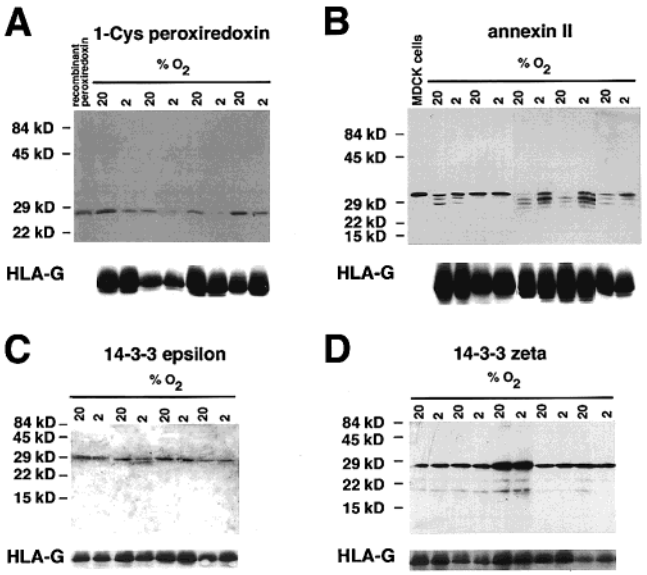

FIGURE 3: Immunoblot analyses confirmed that in cytotrophoblasts the levels of 1-Cys peroxiredoxin and annexin II, but not 14-3-3 epsilon and 14-3-3 zeta, were regulated by oxygen tension. Cell lysates were prepared from cytotrophoblasts that were cultured in either 20 or 2% O_2 for 48 h. (A) Immunoblot analyses confirmed that in four different cell preparations the levels of 1-Cys peroxiredoxin decreased in hypoxia. (B) In contrast, three of the five samples analyzed showed that annexin II levels increased in hypoxia. In this case, many of the cytotrophoblast samples contained multiple bands, not present in the standard MDCK lysates, that were attributable to Dispase treatment during harvesting of the cultured cells. (C and D) As expected from the 2-D PAGE analyses (see Figure 2, panels A and B), expression of neither 14-3-3 epsilon nor 14-3-3 zeta was regulated by oxygen tension. In all cases the blots were stripped and reprobed with an antibody against HLA-G, the cytotrophoblast class I molecule whose abundance does not change in hypoxia. The results, which are shown below each immunoblot, allowed comparison of protein loads within individual experiments (e.g., 20 vs 2% O_2).

3, 13, 14, and 17, appeared at the same position on both maps, but most occupied unique locations (Figure 2, panel C), evidence that suggests the cytotrophoblast protein repertoire reflects the specialized biological functions these cells perform. Finally, we compared the cytotrophoblast 2-D PAGE map to that of the JEG-3 choriocarcinoma cell line. Although these cells have adapted to culture, their protein repertoire (Figure 2, panel D) bore a greater resemblance to that of primary cytotrophoblasts than did that of placental fibroblasts.

MALDI-TOF MS/PSD. Our ultimate goal is to determine the identity of all the protein spots that are visible in Figure 2, panel A. To date, we have used mass spectrometry approaches, primarily MALDI-TOF, to identify 43 different spots. The results of the entire analysis are summarized in Table 1, where spot numbers, marked on the gel in Figure 2, panel A, are correlated with protein identity. Peptides that were subjected to PSD analysis appear in bold, italicized font. Peptide mass fingerprints and peptide fragment-ions were used in database searches to identify the protein. The amino acid positions in the protein sequence of the peptide masses identified are also shown in the table. The mass accuracy of tryptic peptides was in the range of $\pm$ 0.05 Da.

The majority of proteins could be organized into functional groupings. These included the antioxidants manganese superoxide dismutase (Mn SOD), 1-Cys peroxiredoxin, and antioxidant enzyme (AOE) 37-2. Several enzymes in the glycolytic pathway were also identified. With regard to protein chaperones, we detected HSP 27, HSP 70, and GRP-94 (the endoplasmic reticulum form of HSP 90), and molecules that mediate protein folding—protein disulfide isomerase (PDI), PDI-related proteins, ERp28, and cyclophilin. We also found four members of the annexin family of phospholipid-binding proteins. Calcium-binding proteins included calreticulin and calumenin. Finally, we found that three members of the 14-3-3 family of adapter/signaling molecules were among the prominent Coomassie blue-stained spots.

Functional Proteomics: The Effects of Hypoxia on the Cytotrophoblast Protein Repertoire. We were interested in the effects of hypoxia in vitro on cytotrophoblast protein expression as monitored by 2-D PAGE. Visual comparison of the maps of cytotrophoblasts maintained under standard and hypoxic conditions, Figure 2, panels A and B, respectively, showed that the intensity of relatively few protein spots changed when the oxygen tension was reduced to 2%. This finding is in agreement with our previous work that suggests these cells are unusually resistant to the effects of hypoxia, which in fact causes them to proliferate (*12*, *13*). We used the Pharmacia ImageMaster 2D system to compare the intensities of protein spots whose abundance appeared to be regulated by oxygen tension. This analysis showed that of the 250 spots, only six changed in abundance by 2-fold or greater. Levels of four proteins increased as indicated: triosephosphate isomerase (2-fold), phosphoglycerate mutase (2-fold), annexin II (2-fold), and tropomyosin (2-fold). In contrast, levels of two antioxidants decreased: 1-Cys peroxiredoxin (3-fold) and Mn SOD (2-fold). Together, these results suggest that hypoxia exerts discrete effects on the cytotrophoblast protein repertoire; the abundance of most proteins on the 2-D PAGE map did not change.

Immunoblot Analyses of Cytotrophoblast Expression of 1-Cys Peroxiredoxin, Annexin II, 14-3-3 Epsilon, and 14-3-3 Zeta. We used immunoblotting to confirm the identity and oxygen regulation (or lack thereof) of four cytotrophoblast proteins identified by MALDI-TOF MS/PSD. We analyzed the expression of one protein that was downregulated in hypoxia (1-Cys peroxiredoxin), one protein that was upregulated in hypoxia (annexin II) and, as controls, two members of the 14-3-3 family whose levels were not influenced by oxygen tension. Figure 3, panel A shows the results of immunoblotting with anti-1-Cys peroxiredoxin. A single band of the expected size (26 kD) was detected in the lane that contained the recombinant protein. In four separate experiments, hypoxia induced a 2- to 8-fold reduction in cytotrophoblast levels of 1-Cys peroxiredoxin. This was in contrast to the results of immunoblotting with anti-HLA-G, which was used here and subsequently to compare within individual experiments the protein load of lysates prepared from control (20% O_2) and experimental cytotrophoblasts (2% O_2).

Figure 3, panel B, shows the results of immunoblotting with anti-annexin II. The antibody detected a single band of 38 kD in a MDCK cell lysate that served as a positive control. Likewise, cytotrophoblast lysates prepared from cells that were not treated with Dispase also contained a single band (data not shown). In contrast, most of the lysates prepared from Dispase-treated cells contained multiple

Table 1: Summary of MS Analyses of Cytotrophoblast Proteins Identified from 2-D Gels

spot	protein (MW)	% coverage	position of the amino acids of the tryptic peptides in the protein sequence
			Proteins that Function as Antioxidants
2	superoxide dismutase (Mn) (24,722.2)	30	54−68, 76−89, ***115−12***[a], 124−130, ***195−202***,[a] 203−216
1	1-Cys peroxiredoxin (25,035.1)	29	***2−22***[a], ***98−106***[a], 133-141, 133−142, ***145−155***[a], ***156−162***[a]
42	antioxidant enzyme 37-2 (30,540.1)	30	46−66, 48−66, 166−173[b], 174−186, 187−200, 213−223[b], 224−230, 231−240
			Proteins that Function in Glycolysis
5	glyceraldehyde-3-phosphate dehydrogenase (GAPDH) (36,053.3)	27	***67−80***[a], 108-117, 201−215, 201−219, ***228−234***[a,c], 235-248, 310−323
8	triosephosphate isomerase (26,669.6)	27	19−33, 20−33, 70−85[b], 101−113, 176−188, 195−206
9	phosphoglycerate mutase (28,804.1)	15	91−100, 181−191, 223−240[c]
11	enolase (47,169.2)	21	***33−50***[a], 16-28, 184-193, 240−253[c], 270-281, 307-326, 407−412
33	phosphoglycerate kinase (43,967.2)	18	31−39, ***157−171***[a], ***201−216***[a], 280−297
34	aldolase (39,289.0)	33	1−12, ***14−21***[a], 42−55, ***60−68***[a,b], 87−98, 111-133, 153−172[c], 243−257[c], 322−329
			Proteins that Act as Chaperones/Mediators of Protein Folding
40	heat shock protein 27 (22,782.6)	14	***28−37***[a], ***172−188***[a]
23	BiP (HSP 70 family) (72,160.0)	45	50−60, 61−74, 82−96, 102−113, 124−138, ***165−181***[a], 186−197[c], 198−213, 198−214, 262−268[c], 289−306[b], 325−336[c], 327−336[c], 353−367, 354−367, 465−474, ***475−492***[a], 524−532, 533−540, 563−573, 602−617, 622−633, 633−653
22	glucose regulated protein-94 (GRP-94) (92,469.3)	23	***52−67***[a], 76-84, 117-135,143−156[c], 253−265, ***385−395***[a], 396−404, 416−428[c], 475−486, 494−503, 512−530, 538−547[c], 547−557, 548−557, 742−753
12	protein disulfide isomerase (PDI) (56,679.6)	31	63−73, 108−119, 153−173, 259−271, 297−304, 306−329, 352−362, 380−395, 434−448[c], 472-482, 483-496
16	prolyl 4-hydroxylase beta-subunit/ PDI precursor (57,116.6)	33	32−42, ***82−97***[a], 121−130, 196−207, 223−230, 231−247, 255−263, 286−300, 301−308, 317−326[c], 327−338, 376−385, 410−424, ***445−452***[a], 453−461
27	protein disulfide isomerase related protein-5 (46,199.1)	38	1−18, 67−83, 90−99, 100−113, 141−153, 142−153, 176−189, 198−212, 227−237, 295−303, 355−367, 368−373, 374−390, 391−396
3	cyclophilin (22,611.3)	38	37−42, 51−58, 63−75, 90−100[c], 114−120, 137−149, 163−171[c], 196−206
41	ERp 28 (28,993.6)	26	60−69, 110−122, ***113−122***[a], 123−137, 198−204, ***209−223***[a,c], 244−253
			Proteins that Bind Phospholipids
7	annexin I (38,714.5)	34	59−71, 82−98, 99−113, 114−124, 129−144, 167−177, 189−204, 215−212, 215−228
4	annexin II (38,604.2)	16	***29−37***[a], ***50−63***[a], 69−77[b], 136−145, 158−168
32	annexin II (38,604.2)	34	50−63, 69−77[b,] 89−104, 136−145, 179−196, 180−196, 213−220[c], 234−245, 314−324
39	annexin IV (35,882.9)	38	***1−24***[a,c], ***29−44***[a], 142−150, ***144−155***[a,c], 173−184[b], 173−185[b], 193−202, 254−270[c], 276−284[c]
17	annexin V (35,804.8)	51	***6−17***[a], 29-44, 63-75, 79−88[c], 89−96, 108−116, 151−160[c], 193−200, 212−226[c], 227−241, 245−259[c], 260−270, 276−284, 289−300[c], 290−300[c]
			Proteins that Bind Calcium
15	calreticulin (48,141.8)	47	***25−36***[a], 65−73, 74−87, 88−98, 99−111, 143−151, 144−151, 208−222, 273−278, 279−286, 359−366
31	calumenin (37,072.9)	24	38−59, 104−111, 235−241, 256−271, 288−311, 293−311
			Proteins Involved in Signaling
20	14-3-3 epsilon (29,174.1)	33	11−23[c], ***24−31***[a], 112−122, 135−151[c], ***178−196***[a], ***197−206***[a,c]
21	14-3-3 zeta (27,745.3)	44	***28−41***[a], 84−91, 104−115, 121−127[c], 128−139, 140−157, 158−167[c], 159−167[c], 194−212, 213−222[c]
38	14-3-3 gamma (28,374.6)	10	***29−42***[a], ***216−225***[a,c]
			Proteins that Function in Cell Motility or Structure
18	tropomyosin (32,876.1)	29	13−21, 52−65, 137−149[c], 141−152[c], 168−178, 169−178, 183−191, 192−198, 192−201, 218−226
19	tropomyosin (28,522.0)	14	13−27, 14−27, 55−64, 55−65, 132−142, 133−142
13	actin (41,813.1)	14	62−68, ***197−206***[a], ***313−328***[a], 329−335, 360−372[b]
14	actin (41,813.1)	14	178−191[c], 197−206, 313−328, 360−372
26	actin (41,813.1)	18	85−95, 96−113, 197−206, 313−328, 360−372[b]
24	cytokeratin 8 (53,562.3)	30	134−148[c], 161−176[c], 187−197[c], 214−225, 226−233, 234−252[c], 286−295, 329−341, 342−352, 382−392
25	cytokeratin 8 (53,562.3)	15	214−225, 226−233, 329−341, 342−352, 382−392
28	cytokeratin 18 (47,334.2)	38	7−14, 82−90[c], 91−97, 125−131, 132−137, 138−149, 150−158, 159−165, 176−186[b], 197−214[c], 223−241, 254−261, 302−314[c], 318−325, 359−370[b], 371−381, 373−381
29	cytokeratin 19 (44,106.2)	54	82−90[c], 112−118, 114−125, 126−138, 141−150, 151−159, 167−176, 169−176, 177−187[c], 189−197, 198−215[c], 217−226, 227−247, 254−264[c], 266−274, 281−293[c], 318−330, 331−353, 359−365[b], 371−381, 373−381
30	cytokeratin 8 (53,562.3)	43	111−117, 134−148[c], 161−176[c], 179−186, 187−197[c], 214−225, 226−233[b], 234−252[c], 253−264[c], 265−273, 276−285[c], 286−295, 305−312[c], 317−325, 329−341, 342−352, 373−381, 382−392
35	cytokeratin 8 (53,562.3)	23	179−186, 187−197[c], 214−225, 226−233[b], 234−252[c], 329−341, 342−352, 382−392
36	cytokeratin 19 (44,106.2)	32	8−24[b], 25−32, 126−138, 151−159, 167−176, 169−176, 189−197, 217−226, 254−264[c], 281−293, 318−330, 359−365[b], 371−381
			Others
6	aldose reductase (35,853.6)	19	34−41, ***70−78***[a], 156−177[c], 244-251, 252−256[c], 309−316
10	carbonic anhydrase (29,218.1)	13	***81−89***[a], 133−148, 172−181
37	nuclear chloride ion channel (26,923.4)	15	96−113, ***196−204***[a], 209−216
43	glutathione-*S*-transferase (23,224.8)	31	***1−11***[a], 4−11, 55−70, 82−100, 121−140

[a] Bold italicized peptides were analyzed by PSD. [b] Peptide contains an N-terminal pyro-glutamic acid. [c] Peptide contains an oxidized methionine.

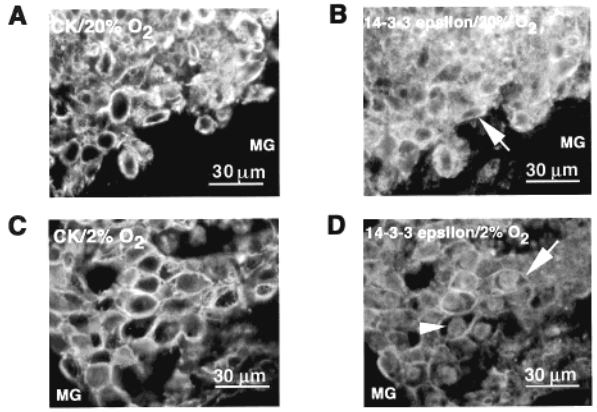

FIGURE 4: Immunolocalization showed that in cultured cytotrophoblasts hypoxia induced translocation of 14-3-3 epsilon to the nucleus. Cytotrophoblasts were cultured for 48 h, then fixed together with the Matrigel (MG) substrate as described in Materials and Methods. Sections of cells that were maintained in either 20% O_2 (A and B) or 2% O_2 (C and D) were stained with antibodies that specifically reacted with cytokeratin, a trophoblast marker (A and C), and 14-3-3 epsilon (B and D). In 20% O_2, 14-3-3 staining primarily localized to the plasma membrane region of the cell (arrow), although some antibody reactivity was also detected in the cytoplasm. In hypoxia, 14-3-3 epsilon expression was detected in association with both the plasma membrane (arrow) and the nucleus (arrowhead). In contrast, expression of 14-3-3 zeta, which was essentially the same as the staining pattern shown in panel B, did not change in hypoxia (data not shown).

immunoreactive bands, likely due to proteolysis of the antigen. Therefore, quantitation was accomplished by summing the signals from all the bands. These results showed that in three of five experiments, annexin II levels rose between 2- and 5-fold in hypoxia, suggesting that this response was somewhat less consistently observed in individual cytotrophoblast preparations than the downregulation of 1-Cys peroxiredoxin expression.

Next, we performed immunoblot analyses of two members of the 14-3-3 family. Anti-14-3-3 epsilon reacted with a single band of the expected size (29 kD) in all the cytotrophoblast lysates except one sample that contained a doublet (Figure 3, panel C). The levels of this antigen did not change in hypoxia. Likewise, anti-14-3-3 zeta primarily reacted with a protein of the expected size (28 kD), and the levels were not affected by a reduction in oxygen tension (Figure 3, panel D). Taken together, the results of the immunoblot analyses confirmed those obtained using the 2-D PAGE/MS approach.

Hypoxia Alters the Subcellular Localization of 14-3-3 Epsilon, but Not 14-3-3 Zeta. Finally, we investigated whether the subcellular localization, rather than the abundance, of the 14-3-3 signaling and adapter proteins changed in hypoxia. Immunolocalization experiments were performed on sections cut from cytotrophoblasts cultured on Matrigel plugs in either a 20% or a 2% O_2 atmosphere (see Materials and Methods). The results are shown in Figure 4. The sections were stained with anti-cytokeratin to confirm that the cells were cytotrophoblasts (CK, Figure 4, panels A and C). In 20% O_2, staining for 14-3-3 epsilon was primarily detected in association with the plasma membrane region of the cells (Figure 4, panel B, denoted by arrow). In 2% O_2, many of the cytotrophoblasts showed nuclear staining (Figure 4, panel D, denoted by arrowhead) in addition to plasma membrane antibody reactivity (denoted by arrow). In contrast, the staining pattern for 14-3-3 zeta, which was also plasma membrane associated, was the same whether the cells were maintained in 2 or 20% O_2 (data not shown). To our knowledge this is the first evidence that 14-3-3 proteins translocate to the nucleus in hypoxia, possible evidence that they play a functional role in cellular responses to reduced oxygen tension.

DISCUSSION

2-D PAGE maps of proteins isolated from other cellular compartments of the human term placenta have been published. These include the microvillus membranes of a different trophoblast population—multinucleate syncytiotrophoblasts that cover the chorionic villi (see Figure 1, panels A and B). Although the identity of most of the spots was not determined, the overall pattern was very different from that of our cytotrophoblast map (*25*). In contrast, an approach very similar to the one we applied, 2-D PAGE combined with protein spot identification by mass spectrometry, was used to map the proteome of mitochondria isolated from whole term placenta (*26*). Since the cytotrophoblast stem cell population is largely depleted at the time of delivery, this preparation likely reflects the protein composition of mitochondria from other placental cell types, primarily fibroblasts and syncytiotrophoblasts (see Figure 1, panels A and B). Thus, it is not surprising that the cytotrophoblast proteome was also distinct from that of placental mitochondria.

The identification of protein gel spots in 2-D PAGE maps of cytotrophoblasts maintained under standard tissue culture conditions revealed high abundance proteins that are commonly found in all cells, as well as particular specializations. The former category included tropomyosin, cytokeratin, and actin isoforms. Since term placenta is often used as a source of human proteins and RNA, the latter category included proteins that were already known to be expressed somewhere in this organ. However, only a subset has been localized to the specialized invasive cytotrophoblast population that was the subject of this study. For example, we were intrigued to find that abundant antioxidants included 1-Cys peroxiredoxin and AOE 37-2, in addition to Mn SOD, whose expression in human trophoblasts has been well studied (*27*). Experiments to localize protein and mRNA have shown that 1-Cys peroxiredoxin is highly expressed in organs exposed to high oxygen levels, such as skin and lung (*17*, *28*). This finding correlates well with the protein's function as an antioxidant. Interestingly, 1-Cys peroxiredoxin expression reduces phospholipid hydroperoxides and may thus play a vital role in defending the plasma membrane against the effects of oxidative stress (*29*).

Similarly, we expanded the list of heat shock and chaperone proteins known to be expressed in cytotrophoblasts to include GRP-94, the endoplasmic reticulum homologue of HSP 90 that controls expression of the epidermal growth factor receptor (*30*). Cyclophilin, which possesses enzymatic peptidyl-prolyl isomerase activity that is essential for protein folding, was also abundant. Clearly, the annexins are also among the major cytotrophoblast proteins. Finally, in keeping with their high glycogen content, enzymes that are involved in glycolysis are among the most abundant proteins in the cells.

We also examined the effects of hypoxia (2% O_2) on the first trimester human cytotrophoblast proteome. The reason

for focusing on this variable was our past work showing that oxygen tension is an important regulator of cytotrophoblast differentiation/invasion. This relationship may reflect the fact that the placenta is the first organ to function during development. As a result, the initial stages of placental development occur before the conceptus accesses a supply of maternal blood, ≤10 weeks of gestation (*31*). In accord with this constraint, our previous work shows that cytotrophoblasts proliferate in vitro under hypoxic conditions that are comparable to those found during early pregnancy in the uterine lumen and the superficial decidua (2% O_2). As trophoblast invasion of the uterus and its resident blood vessels proceeds, the placental cells encounter increasingly higher oxygen levels (*32*), which trigger their exit from the cell cycle and subsequent differentiation (*12*). Very recently, we have explained the unusual response of cytotrophoblasts to hypoxia in terms of the known regulators of oxygen-dependent cellular responses. Specifically, hypoxia induces cytotrophoblast expression of the von Hippel-Lindau tumor suppressor protein, which targets hypoxia-inducible factors for ubiquitination and degradation (Genbacev et al., unpublished data). Thus, the placenta appears to have evolved highly specialized mechanisms for protecting itself against the usual spectrum of hypoxia-induced changes in cellular protein expression.

In accord with this observation, we found that hypoxia produced very few changes in the expression of cytotrophoblast proteins; some were anticipated and others could not have been predicted. As expected, we did see changes in the abundance of proteins that are involved in glycolysis and in mitigating the effects of oxidative stress. With regard to glycolysis, we observed an increase in the expression of triosephosphate isomerase and phosphoglycerate mutase. This result is consistent with hypoxia-induced increases in glycolysis that have been observed in other systems, including endothelial cells (*33*), and with increased glucose consumption by human term cytotrophoblasts in response to hypoxia (*34*). We also expected changes in the levels of antioxidants. In fact, the expression of two such proteins, Mn SOD and 1-Cys peroxiredoxin, decreased. The fall in SOD levels is consistent with our previous finding that the in situ expression of the Cu/Zn form of this enzyme is downregulated in invasive cytotrophoblasts in preeclampsia, a pregnancy complication that is thought to occur as a consequence of placental hypoxia (*35*). Increasing evidence indicates that reactive oxygen species (ROS) play a role in signaling pathways and gene transcription (*36*, *37*). Therefore, identifying changes in the levels of the proteins that modulate levels of ROS may help to unravel pathways involved in the etiology of this syndrome.

Other changes in the observed cytotrophoblast response to reduced oxygen tension were unexpected. With regard to changes in protein abundance, we were surprised to see that the expression of both annexin II and tropomyosin was upregulated by hypoxia. Annexins are a family of calcium- and phospholipid-binding proteins with multiple functions (*38*). With regard to the consequences of increased cytotrophoblast expression of annexin II in hypoxia, several possibilities exist. In other cells, annexin II levels correlate with proliferative capacity (*39*). Our results suggest that this relationship may also hold true in cytotrophoblasts. Additionally, the ability of annexin II to control fibrinolysis in endothelial cells (*40*) may suggest a parallel function in invasive cytotrophoblasts, which have many vascular-like properties. Clearly, limiting fibrin deposition at sites where cytotrophoblasts interface with maternal blood (see Figure 1, panels A and B) is a critical determinant of the outcome of pregnancy. Likewise, an increase in tropomyosin expression in response to hypoxia has been observed in arterial endothelial cells, although the functional significance of this observation is not yet understood (*41*).

Finally, the relative abundance in cytotrophoblasts of certain members of the 14-3-3 protein family prompted us to use additional methods to search for hypoxia-induced changes in their expression. Immunoblotting analyses confirmed that both 14-3-3 epsilon and zeta migrated as single bands on 1-D gels and that their abundance was not influenced by oxygen tension. In contrast, immunolocalization showed that the epsilon, but not the zeta species, moved to the nucleus in hypoxia. Although the precise consequences of this translocation are not known, we assume that this observation is indicative of oxygen-regulated interactions between 14-3-3 epsilon and a subset of proteins to which it binds. These include components of intracellular pathways that influence processes such as transcription (*42*), passage through the cell cycle (*43*), signal transduction (*44*, *45*), and cell adhesion (*46*).

Together these results, combined with information about the effects of hypoxia, give us new insights into how these unusual cells respond to the changes in oxygen tension that normally occur during the first trimester of pregnancy. In addition, a subset of these molecules could be used as markers to aid in unraveling the etiology of pregnancy complications that have been linked to placental hypoxia. These studies are now in progress.

ACKNOWLEDGMENT

We thank Evangeline Leash for excellent editorial assistance.

REFERENCES

1. Norwitz, E. R., and Repke, J. T. (2000) *J. Soc. Gynecol. Invest. 7*, 21−36.
2. Meekins, J. W., Pijnenborg, R., Hanssens, M., McFadyen, I. R., and van Asshe, A. (1994) *Br. J. Obstet. Gynaecol. 101*, 669−674.
3. Friedman, S. A., Taylor, R. N., and Roberts, J. M. (1991) *Clin. Perinatol. 18*, 661−682.
4. Roberts, J. M., and Redman, C. W. (1993) *Lancet 341*, 1447−1451.
5. Cross, J. C. (1998) *Ann. N. Y. Acad. Sci. 857*, 23−32.
6. Janatpour, M. J., McMaster, M. T., Genbacev, O., Zhou, Y., Dong, J., Cross, J. C., Israel, M. A., and Fisher, S. J. (2000) *Development 127*, 549−558.
7. Janatpour, M. J., Utset, M. F., Cross, J. C., Rossant, J., Dong, J., Israel, M. A., and Fisher, S. J. (1999) *Dev. Genet. 25*, 146−157.
8. Damsky, C. H., and Fisher, S. J. (1998) *Curr. Opin. Cell Biol. 10*, 660−666.
9. Librach, C. L., Werb, Z., Fitzgerald, M. L., Chiu, K., Corwin, N. M., Esteves, R. A., Grobelny, D., Galardy, R., Damsky, C. H., and Fisher, S. J. (1991) *J. Cell Biol. 113*, 437−449.
10. McMaster, M. T., Librach, C. L., Zhou, Y., Lim, K. H., Janatpour, M. J., DeMars, R., Kovats, S., Damsky, C., and Fisher, S. J. (1995) *J. Immunol. 154*, 3771−3778.
11. Zhou, Y., Damsky, C. H., and Fisher, S. J. (1997) *J. Clin. Invest. 99*, 2152−2164.

12. Genbacev, O., Joslin, R., Damsky, C. H., Polliotti, B. M., and Fisher, S. J. (1996) *J. Clin. Invest. 97*, 540−550.
13. Genbacev, O., Zhou, Y., Ludlow, J. W., and Fisher, S. J. (1997) *Science 277*, 1669−1672.
14. Hui, P., Parkash, V., Perkins, A. S., and Carcangiu, M. L. (2000) *Lab. Invest. 80*, 965−972.
15. Cross, J. C. (2000) *Semin. Cell Dev. Biol. 11*, 105−113.
16. Tanaka, T. S., Jaradat, S. A., Lim, M. K., Kargul, G. J., Wang, X. H., Grahovac, M. J., Pantano, S., Sano, Y., Piao, Y., Nagaraja, R., Doi, H., Wood, W. H., Becker, K. G., and Ko, M. S. H. (2000) *Proc. Natl. Acad. Sci. U.S.A. 97*, 9127−9132.
17. Novoselov, S. V., Peshenko, I. V., Popov, V. I., Novoselov, V. I., Bystrova, M. F., Evdokimov, V. J., Kamzalov, S. S., Merkulova, M. I., Shuvaeva, T. M., Lipkin, V. M., and Fesenko, E. E. (1999) *Cell Tissue Res. 298*, 471−480.
18. Damsky, C. H., Fitzgerald, M. L., and Fisher, S. J. (1992) *J. Clin. Invest. 89*, 210−222.
19. Genbacev, O., Schubach, S. A., and Miller, R. K. (1992) *Placenta 13*, 439−461.
20. Genbacev, O., Jensen, K. D., Powlin, S. S., and Miller, R. K. (1993) *Placenta 14*, 463−475.
21. Fisher, S. J., Cui, T. Y., Zhang, L., Hartman, L., Grahl, K., Zhang, G. Y., Tarpey, J., and Damsky, C. H. (1989) *J. Cell Biol. 109*, 891−902.
22. Bradford, M. M. (1976) *Anal. Biochem. 72*, 248−254.
23. Matsui, N. M., Smith, D. M., Clauser, K. R., Fichmann, J., Andrews, L. E., Sullivan, C. M., Burlingame, A. L., and Epstein, L. B. (1997) *Electrophoresis 18*, 409−417.
24. Clauser, K. R., Baker, P., and Burlingame, A. L. (1999) *Anal. Chem. 71*, 2871−2882.
25. Webb, P. D., Evans, P. W., Molloy, C. M., and Johnson, P. M. (1985) *Am. J. Reprod. Immunol. Microbiol. 8*, 113−119.
26. Rabilloud, T., Kieffer, S., Procaccio, V., Louwagie, M., Courchesne, P. L., Patterson, S. D., Martinez, P., Garin, J., and Lunardi, J. (1998) *Electrophoresis 19*, 1006−1014.
27. Church, S. L., Farmer, D. R., and Nelson, D. M. (1992) *Dev. Biol. 149*, 177−184.
28. Kim, T. S., Dodia, C., Chen, X., Hennigan, B. B., Jain, M., Feinstein, S. I., and Fisher, A. B. (1998) *Am. J. Physiol. 274*, L750−761.
29. Fisher, A. B., Dodia, C., Manevich, Y., Chen, J. W., and Feinstein, S. I. (1999) *J. Biol. Chem. 274*, 21326−21334.
30. Supino-Rosin, L., Yoshimura, A., Yarden, Y., Elazar, Z., and Neumann, D. (2000) *J. Biol. Chem. 275*, 21850−21855.
31. Burton, G. J., Jauniaux, E., and Watson, A. L. (1999) *Am. J. Obstet. Gynecol. 181*, 718−724.
32. Pijnenborg, R., Robertson, W. B., Brosens, I., and Dixon, G. (1981) *Placenta 2*, 71−91.
33. Graven, K. K., Troxler, R. F., Kornfeld, H., Panchenko, M. V., and Farber, H. W. (1994) *J. Biol. Chem. 269*, 24446−24453.
34. Esterman, A., Greco, M. A., Mitani, Y., Finlay, T. H., Ismail-Beigi, F., and Dancis, J. (1997) *Placenta 18*, 129−136.
35. Many, A., Hubel, C. A., Fisher, S. J., Roberts, J. M., and Zhou, Y. (2000) *Am. J. Pathol. 156*, 321−331.
36. Servitja, J. M., Masgrau, R., Pardo, R., Sarri, E., and Picatoste, F. (2000) *J. Neurochem. 75*, 788−794.
37. Khan, A. U., and Wilson, T. (1995) *Chem. Biol. 2*, 437−445.
38. Raynal, P., and Pollard, H. B. (1994) *Biochim. Biophys. Acta 1197*, 63−93.
39. Menaa, C., Devlin, R. D., Reddy, S. V., Gazitt, Y., Choi, S. J., and Roodman, G. D. (1999) *J. Clin. Invest.103*, 1605−1613.
40. Hajjar, K. A., and Acharya, S. S. (2000) *Ann. N. Y. Acad. Sci. 902*, 265−271.
41. Rao, U. J., Denslow, N. D., and Block, E. R. (1994) *Am. J. Physiol. 267*, L271−281.
42. Brunet, A., Bonni, A., Zigmond, M. J., Lin, M. Z., Juo, P., Hu, L. S., Anderson, M. J., Arden, K. C., Blenis, J., and Greenberg, M. E. (1999) *Cell 96*, 857−868.
43. Peng, C. Y., Graves, P. R., Thoma, R. S., Wu, Z., Shaw, A. S., and Piwnica-Worms, H. (1997) *Science 277*, 1501−1505.
44. Fu, H., Xia, K., Pallas, D. C., Cui, C., Conroy, K., Narsimhan, R. P., Mamon, H., Collier, R. J., and Roberts, T. M. (1994) *Science 266*, 126−129.
45. Hausser, A., Storz, P., Link, G., Stoll, H., Liu, Y. C., Altman, A., Pfizenmaier, K., and Johannes, F. J. (1999) *J. Biol. Chem. 274*, 9258−9264.
46. Garcia-Guzman, M., Dolfi, F., Russello, M., and Vuori, K. (1999) *J. Biol. Chem. 274*, 5762−5768.
47. Zhou, Y., Damsky, C. H., Chiu, K., Roberts, J. M., and Fisher, S. J. (1993) *J. Clin. Invest. 91*, 950−960.

BI0023910